Structure and Physical Properties of Ternary Antimonide $YbCrSb_3$

Shane J. Crerar, Laura Deakin, and Arthur Mar*

Department of Chemistry, University of Alberta, Edmonton, Alberta, Canada T6G 2G2

Received March 21, 2005. Revised Manuscript Received March 31, 2005

The ternary rare-earth antimonide $YbCrSb_3$ was prepared by arc-melting of the elements. Its structure was determined by single-crystal X-ray diffraction (Pearson symbol *oP*20, orthorhombic, space group *Pbcm*, $Z = 4$, $a = 12.981(3)$ Å, $b = 6.140(1)$ Å, $c = 5.993(1)$ Å). $YbCrSb_3$ is isostructural to $LaCrSb_3$ and $CeCrSb_3$, and extends the $RECrSb_3$ series (previously known for *RE* = La, Ce, Pr, Nd, Sm, Gd, Tb, Dy) to the latest rare-earth member yet and to one that is essentially divalent instead of trivalent. Electrical resistivity measurements on single crystals and magnetic susceptibility measurements on powders revealed a magnetic ordering transition at $T_C = \sim 280$ K, the highest observed so far in the $RECrSb_3$ series. The isothermal magnetization at 100 K indicated an approach to saturation, but with low values (0.08 μ_B/mol at 9 T). These results suggest a ferromagnetic or canted antiferromagnetic structure.

Introduction

An extensive series of ternary rare-earth (*RE*) chromium antimonides, $RECrSb_3$, was first discovered by Brylak and Jeitschko for the early rare earths (*RE* = La, Ce, Pr, Nd, Sm)[1] and subsequently extended by us to the late rare earths (*RE* = Gd, Tb, Dy).[2] They adopt a crystal structure with strongly two-dimensional character imparted by the presence of Sb square nets, a substructure now being recognized as common to many Sb-rich compounds.[3] As with many intermetallic compounds consisting of rare-earth and transition metals, these antimonides exhibit varied electrical and magnetic properties arising from the interaction of f and d electrons.

The prototype compound, $LaCrSb_3$, displays ferromagnetic ordering[4−9] at $T_C = \sim 120-140$ K and a spin-reorientation transition at $T_{sr} = \sim 95$ K.[10] It has been intensely studied because the absence of f electrons in La^{3+} implies that any magnetic ordering originates entirely from Cr d electrons, so it serves as a reference to which other $RECrSb_3$ members may be compared. There is ongoing debate about the nature of the metallic magnetism and whether there is a coexistence of localized and itinerant spins in $LaCrSb_3$.[10−12] For other $RECrSb_3$ members (*RE* = Ce, Pr, Nd, Sm), the presence of f electrons on the *RE* atoms leads to the appearance of a second ordering transition at lower temperatures ($T_C = 10-30$ K).[4,6,7,13,14] The transition temperatures scale with the de Gennes factor, consistent with strong interactions between f and d electrons, to the extent that they converge to a single ferrimagnetic transition for $GdCrSb_3$ ($T_C = \sim 90$ K).[15,16]

There has been impetus to study the later rare-earth members of the $RECrSb_3$ series, which to date have been prepared for up to *RE* = Dy. Crystal chemical considerations suggest that severe bond strain develops as substitution with a smaller *RE* atom contracts the crystal structure.[2] Following up on recently communicated preliminary results,[17] we present here full details on the new compound $YbCrSb_3$, which extends the $RECrSb_3$ series to the latest rare-earth member yet. Because Yb can be either divalent or trivalent, there are important implications for both the crystal and electronic structure. Even more remarkably, $YbCrSb_3$ displays a single magnetic ordering transition at the highest temperature observed so far, $T_C = \sim 280$ K, in the $RECrSb_3$ series.

Experimental Section

Synthesis. Starting materials were powders of Yb (99.9%, Cerac or Alfa-Aesar), Cr (99.95%, Cerac), and Sb (99.995%, Cerac or Alfa-Aesar). $YbCrSb_3$ was originally identified from flux treatment of the product of an arc-melting reaction of Yb, Cr, and Sb in a 2:4:5 molar ratio. A cold-pressed pellet (~0.25 g) was prepared and reacted in an Edmund Bühler MAM-1 compact arc melter on

* To whom correspondence should be addressed. E-mail: arthur.mar@ualberta.ca.

(1) Brylak, M.; Jeitschko, W. *Z. Naturforsch. B: Chem. Sci.* **1995**, *50*, 899−904.
(2) Ferguson, M. J.; Hushagen, R. W.; Mar, A. *J. Alloys Compd.* **1997**, *249*, 191−198.
(3) Mills, A. M.; Lam, R.; Ferguson, M. J.; Deakin, L.; Mar, A. *Coord. Chem. Rev.* **2002**, *233−234*, 207−222.
(4) Hartjes, K.; Jeitschko, W.; Brylak, M. *J. Magn. Magn. Mater.* **1997**, *173*, 109−116.
(5) Raju, N. P.; Greedan, J. E.; Ferguson, M. J.; Mar, A. *Chem. Mater.* **1998**, *10*, 3630−3635.
(6) Leonard, M.; Saha, S.; Ali, N. *J. Appl. Phys.* **1999**, *85*, 4759−4761.
(7) Leonard, M. L.; Dubenko, I. S.; Ali, N. *J. Alloys Compd.* **2000**, *303−304*, 265−269.
(8) Dubenko, I. S.; Hill, P.; Ali, N. *J. Appl. Phys.* **2001**, *89*, 7326−7328.
(9) Jackson, D. D.; Torelli, M.; Fisk, Z. *Phys. Rev. B* **2001**, *65*, 014421.
(10) Granado, E.; Martinho, H.; Sercheli, M. S.; Pagliuso, P. G.; Jackson, D. D.; Torelli, M.; Lynn, J. W.; Rettori, C.; Fisk, Z.; Oseroff, S. B. *Phys. Rev. Lett.* **2002**, *89*, 107204.
(11) Shim, J. H.; Min, B. I. *J. Magn. Magn. Mater.* **2004**, *272−276*, e241−e242.
(12) Richter, M.; Rusz, J.; Rosner, H.; Koepernik, K.; Opahle, I.; Nitzsche, U.; Eschrig, H. *J. Magn. Magn. Mater.* **2004**, 272−276, e251−e252.
(13) Deakin, L.; Ferguson, M. J.; Mar, A.; Greedan, J. E.; Wills, A. S. *Chem. Mater.* **2001**, *13*, 1407−1412.
(14) Jackson, D. D.; Fisk, Z. *J. Magn. Magn. Mater.* **2003**, *256*, 106−116.
(15) Deakin, L.; Mar, A. *Chem. Mater.* **2003**, *15*, 3343−3346.
(16) Jackson, D. D.; Fisk, Z. *J. Alloys Compd.* **2004**, *377*, 243−247.
(17) Tkachuk, A. V.; Crerar, S. J.; Wu, X.; Muirhead, C. P. T.; Deakin, L.; Mar, A. *Mater. Res. Soc. Symp. Proc.* **2005**, *848*, FF2.6.1.

10.1021/cm0506151 CCC: $30.25
Published on Web 04/23/2005

Table 1. Crystallographic Data for $YbCrSb_3$

formula	$YbCrSb_3$
formula mass (amu)	590.29
space group	*Pbcm* (No. 57)
a (Å)	12.981(3)
b (Å)	6.140(1)
c (Å)	5.993(1)
V (Å^3)	477.6(2)
Z	4
ρ_{calcd} (g cm^{-3})	8.209
crystal dimensions (mm)	0.20 × 0.04 × 0.01
radiation	graphite monochromated Mo *K*α, $\lambda = 0.71073$ Å
μ(Mo *K*α) (cm^{-1})	113.97
transmission factors	0.087−0.654
2θ limits	$3.14° \le 2\theta(\text{Mo } K\alpha) \le 66.32°$
data collected	$-19 \le h \le 19$, $-9 \le k \le 9$, $-9 \le l \le 9$
no. of data collected	6074
no. of unique data, including $F_o^2 < 0$	974
no. of unique data, with $F_o^2 > 2\sigma(F_o^2)$	825
no. of variables	29
$R(F)$ for $F_o^2 > 2\sigma(F_o^2)$[a]	0.059
$R_w(F_o^2)$[b]	0.161
GOF	1.173
$(\Delta\rho)_{max}$, $(\Delta\rho)_{min}$ (e Å^{-3})	7.80, −3.19

[a] $R(F) = \sum||F_o| - |F_c||/\sum|F_o|$. [b] $R_w(F_o^2) = [\sum [w(F_o^2 - F_c^2)^2]/\sum wF_o^4]^{1/2}$; $w^{-1} = [\sigma^2(F_o^2) + (0.0920p)^2 + 10.3941p]$ where $p = \{[\max(F_o^2,0) + 2F_c^2]\}/\{3\}$.

a water-cooled copper bottom under an argon atmosphere. To promote growth of suitably sized crystals, the resulting ingot was ground, combined with 0.3 g Sn (which acts as a flux), and placed in an evacuated fused-silica tube. The tube was heated at 1000 °C for 6 h, cooled to 600 °C over 6 h, heated at 600 °C for 24 h, and then cooled to room temperature over 6 h. The Sn flux was removed by treatment with hydrochloric acid, and the crystals, which were generally less than 0.5 mm long, were washed with distilled water. Energy-dispersive X-ray (EDX) analyses on a Hitachi S-2700 scanning electron microscope revealed the presence of Yb, Cr, and Sb, and confirmed that Sn was not incorporated into the product. A crystal identified in this manner was selected for structure determination.

Samples for physical property measurements were prepared similarly but with Yb, Cr, and Sb in a 1:1:3 molar ratio. Single crystals or aggregates of crystals were screened by EDX measurements. For magnetic measurements, single crystals were selected manually and were ground finely into a powder; analysis by powder X-ray diffraction on an Enraf-Nonius FR552 Guinier camera confirmed that these specimens are phase-pure.

Arc-melting of a stoichiometric mixture of Yb, Cr, and Sb followed by annealing at 1000 °C without the addition of a Sn flux yields a microcrystalline powder that consists of $YbCrSb_3$ as the majority phase but with minor amounts of CrSb and Sb. It is important to add an excess of Yb and Sb during the arc-melting reaction to compensate for evaporative losses. The cell parameters refined for the $YbCrSb_3$ phase from these reactions ($a = 12.99(4)$ Å, $b = 6.13(2)$ Å, $c = 5.99(2)$ Å) are in good agreement with those from the single-crystal data (Table 1).

Structure Determination. Intensity data for $YbCrSb_3$ were collected on a Bruker Platform/SMART 1000 CCD diffractometer at 22 °C using ω scans (0.2°). Crystal data and further details of the data collection are given in Table 1. Calculations were carried out with use of the SHELXTL (version 6.12) package.[18] Face-indexed numerical absorption corrections were applied. The centrosymmetric space group *Pbcm* was chosen and initial atomic positions were taken from the structure of $LaCrSb_3$.[2] Refinements proceeded in a straightforward manner. Because partial occupancy has been implicated in previous structure determinations of $LaCr_{0.95(2)}Sb_3$ and $CeCr_{0.901(9)}Sb_{2.909(4)}$,[1,2] the occupancy of each site in $YbCrSb_3$ was refined successively. The occupancies converged to values between 0.99(1) and 1.01(1) for all sites, from which we conclude that $YbCrSb_3$ is fully stoichiometric. The maximum peak and deepest hole are located 0.74 and 0.67 Å, respectively, from Yb. Final values of the positional and displacement parameters are given in Table 2. Interatomic distances are listed in Table 3. Further crystallographic data, in the form of a CIF, are available in the Supporting Information. The CIF has also been sent to Fachinformationszentrum Karlsruhe, Abt. PROKA, 76344 Eggenstein-Leopoldshafen, Germany as supplementary material No. CSD-415273.

(18) Sheldrick, G. M. *SHELXTL*, version 6.12; Bruker AXS Inc.: Madison, WI, 2001.

Table 2. Positional and Equivalent Isotropic Displacement Parameters for $YbCrSb_3$

atom	Wyckoff position	*x*	*y*	*z*	U_{eq} (Å^2)[a]
Yb	4*d*	0.31066(6)	0.0014(1)	1/4	0.0134(2)
Cr	4*c*	0.9018(2)	1/4	0	0.0120(5)
Sb1	4*d*	0.06561(9)	0.1145(2)	1/4	0.0127(3)
Sb2	4*d*	0.2206(1)	0.4898(2)	1/4	0.0131(3)
Sb3	4*c*	0.50211(8)	1/4	0	0.0132(3)

[a] U_{eq} is defined as one-third of the trace of the orthogonalized U_{ij} tensor.

Table 3. Selected Interatomic Distances (Å) in $YbCrSb_3$

Yb−Sb2	3.217(1) (×2)	Cr−Sb2	2.706(2) (×2)
Yb−Sb2	3.219(1)	Cr−Sb1	2.726(1) (×2)
Yb−Sb3	3.246(1) (×2)	Cr−Sb1	2.731(2) (×2)
Yb−Sb1	3.256(2)	Cr−Cr	2.9963(6) (×2)
Yb−Sb3	3.279(1) (×2)	Sb1−Sb2	3.058(2) (×2)
Yb−Sb2	3.352(1)	Sb3−Sb3	2.9963(6) (×2)
Yb−Cr	3.498(2) (×2)	Sb3−Sb3	3.0703(6) (×2)

Electrical and Magnetic Measurements. The electrical resistivity of single crystals of $YbCrSb_3$ was measured by standard four-probe techniques on a Quantum Design PPMS system equipped with an ac transport controller (model 7100) up to 330 K, the high-temperature limit of our instrumentation. The current was 100 μA and the frequency was 16 Hz. The resistivity was measured along the needle axis of the crystal, which corresponds to the crystallographic *c* axis.

Measurements of dc magnetic susceptibility were made on a 19-mg ground sample of $YbCrSb_3$ between 2 and 330 K under zero-field-cooled conditions in an applied field of 5000 Oe on a Quantum Design 9T-PPMS dc magnetometer/ac susceptometer. The susceptibility was corrected for sample and holder diamagnetism. Measurements of ac magnetic susceptibility were made with a driving amplitude of 5 Oe and a frequency of 1000 Hz.

Results

Structure. $YbCrSb_3$ is a new member of the *RE*$CrSb_3$ series, which was previously believed to terminate at *RE* = Dy. A plot of the unit cell volume reveals the expected decrease resulting from the lanthanide contraction on going from *RE* = La to Dy (Figure 1). However, $YbCrSb_3$ deviates from the extrapolated decrease, and in fact, has a unit cell volume that more closely resembles that of $SmCrSb_3$. This observation argues strongly for the presence of divalent Yb, in contrast to trivalent *RE* for all the other members. The

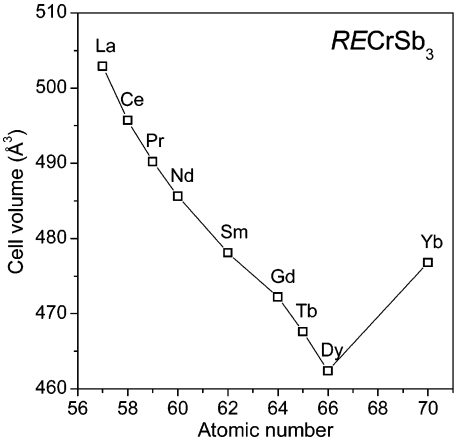

Figure 1. Plot of unit cell volumes for *RE*$CrSb_3$ compounds.

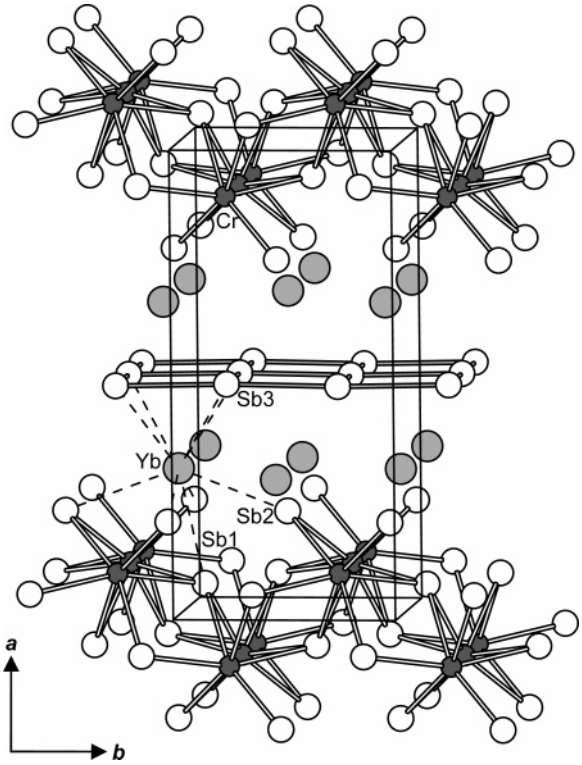

Figure 2. Crystal structure of $YbCrSb_3$ viewed down the *c* axis. The large lightly shaded circles are Yb atoms, the small solid circles are Cr atoms, and the medium open circles are Sb atoms.

ionic radius of Sm^{3+} (crystal radius = 1.27 Å for CN9) is similar to that of Yb^{2+} (~1.33 Å).[19]

The structure of $YbCrSb_3$ is shown in Figure 2. It is built up by inserting Yb atoms between layers of condensed Cr-centered octahedra, $^2_\infty[CrSb_2]$, and nearly square nets of Sb atoms, $^2_\infty[Sb]$, that are stacked along the *a* direction. The Yb atoms are found in nine-coordinate, monocapped square antiprismatic geometry, with Yb−Sb distances ranging from 3.217(1) to 3.352(1) Å. These distances are comparable to those found in other binary and ternary antimonides such as $YbSb_2$ (3.19(1)−3.57(1) Å)[20] and $Yb_5In_2Sb_6$ (3.168(1)−3.546(1) Å)[21] where divalent Yb can be assumed to be present, but are longer than those in YbSb (3.041 Å),[22] which contains essentially trivalent Yb.[23,24] The Cr-centered octahedra share faces along the *c* direction and edges along the *b* direction. The Cr−Sb distances, ranging from 2.706(2) to 2.731(2) Å, appear to be little changed from those in $LaCrSb_3$ and $CeCrSb_3$.[1,2] Indeed, the average Cr−Sb distance is essentially identical in $LaCrSb_3$ (2.72 Å), $CeCrSb_3$ (2.71 Å), and $YbCrSb_3$ (2.72 Å). Similarly, the Sb−Sb distances within the square net in $YbCrSb_3$ (2.9963(6)−3.0703(6) Å) are not significantly different from those in $LaCrSb_3$ (3.0581(5)−3.1065(1) Å) and $CeCrSb_3$ (3.040(1)−3.092(1) Å).

As we had speculated earlier, substitution with a smaller *RE* in the *RE*$CrSb_3$ series cannot proceed indefinitely because of severe bond strain that ensues as the structure contracts.[2] This contraction is not isotropic. The *a* parameter (along the stacking direction) changes considerably more than the *b* and *c* parameters (parallel to the $^2_\infty[CrSb_2]$ layers and $^2_\infty[Sb]$ nets). For example, on going from $DyCrSb_3$ to $YbCrSb_3$, the *a* parameter increases by 8% while the *b* and *c* parameters barely increase by 0.2%. In terms of the crystal structure, the interpretation is that the $^2_\infty[Sb]$ nets remain invariant while the $^2_\infty[CrSb_2]$ layers experience severe buckling in order to maintain reasonable Cr−Sb bond lengths. As the $^2_\infty[CrSb_2]$ layer undulates along the *b* direction, the degree of this buckling can be measured by the Cr−Cr−Cr angle, which decreases from 104.5° in $LaCrSb_3$ to 100.6° in $YbCrSb_3$. The latter value appears to be a lower limit, as the Cr−Cr−Cr angle calculated for $DyCrSb_3$ (assuming atomic coordinates from $YbCrSb_3$) is 102.2°. The resulting distortions are probably very important in influencing the electronic properties of *RE*$CrSb_3$ compounds. The related *RE*$NiSb_3$ structures exhibit severe distortions of Ni-centered octahedra, which seem to be connected with the formation not only of metal−metal bonds, but also of additional Sb−Sb bonds.[25, 26]

Electrical Resistivity. The electrical resistivity of a single crystal of $YbCrSb_3$, measured along the *c* axis as a function of temperature, is shown in Figure 3a. The profile indicates metallic behavior, with absolute resistivities (ρ_{300} = ~110 $\mu\Omega$·cm, ρ_5 = ~10 $\mu\Omega$·cm) similar to those of other *RE*$CrSb_3$ compounds. There is a change in slope, more clearly visible in a plot of the derivative (inset of Figure 3a), that is a recurring feature of all *RE*$CrSb_3$ members examined so far and is attributed to a magnetic ordering transition. The transition in $YbCrSb_3$ occurs at ~280 K, the highest temperature observed so far in the *RE*$CrSb_3$ series. Similar to $LaCrSb_3$ and $SmCrSb_3$,[9,14] the low-temperature resistivity data can be fit to a $T^{3/2}$ dependence, as shown in Figure 3b, that is characteristic of some ferromagnetic metallic systems.

(19) Shannon, R. D. *Acta Crystallogr., Sect. A* **1976**, *32*, 751−767.
(20) Wang, R.; Bodnar, R.; Steinfink, H. *Inorg. Chem.* **1966**, *5*, 1468−1470.
(21) Kim, S.-J.; Ireland, J. R.; Kannewurf, C. R.; Kanatzidis, M. G. *J. Solid State Chem.* **2000**, *155*, 55−61.
(22) Bodnar, R. E.; Steinfink, H. *Inorg. Chem.* **1967**, *6*, 327−330.
(23) Li, D. X.; Oyamada, A.; Hashi, K.; Haga, Y.; Matsumura, T.; Shida, H.; Suzuki, T.; Kasuya, T.; Dönni, A.; Hulliger, F. *J. Magn. Magn. Mater.* **1995**, *140−144*, 1169−1170.
(24) Svane, A.; Temmerman, W. M.; Szotek, Z.; Petit, L.; Strange, P.; Winter, H. *Phys. Rev. B* **2000**, *62*, 13394−13399.
(25) Macaluso, R. T.; Wells, D. M.; Sykora, R. E.; Albrecht-Schmitt, T. E.; Mar, A.; Nakatsuji, S.; Lee, H.; Fisk, Z.; Chan, J. Y. *J. Solid State Chem.* **2004**, *177*, 293−298.
(26) Thomas, E. L.; Macaluso, R. T.; Lee, H.-O.; Fisk, Z.; Chan, J. Y. *J. Solid State Chem.* **2004**, *177*, 4228−4236.

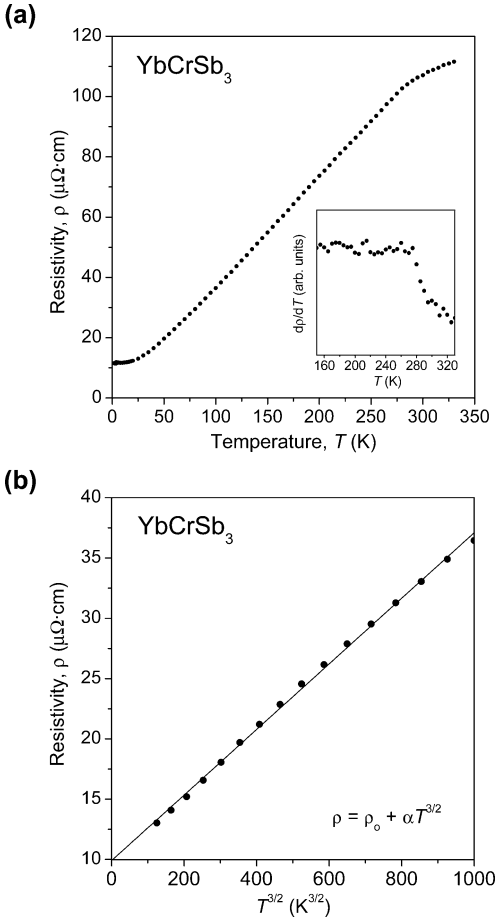

Figure 3. (a) Electrical resistivity measured along the needle axis (parallel to the *c* direction) of a single crystal of $YbCrSb_3$. The inset shows a plot of the derivative near the transition at $T_C = \sim 280$ K. (b) Fit of the low-temperature resistivity data to a $T^{3/2}$ dependence.

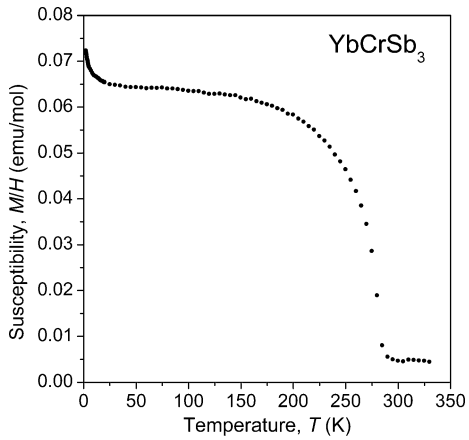

Figure 4. Zero-field-cooled dc magnetic susceptibility of a powder sample of $YbCrSb_3$ ($H_{dc} = 5000$ Oe).

Magnetic Properties. The zero-field-cooled dc magnetic susceptibility of a polycrystalline sample of $YbCrSb_3$ is shown in Figure 4. The effective magnetic moment at 300 K is 3.36 μ_B/f.u., but any simple interpretation of this value in terms of localized Yb^{2+} and Cr^{3+} ions is problematic, as with other *RE*$CrSb_3$ members. A rapid increase in the susceptibility, characteristic of long-range ferromagnetic ordering, occurs below $T_C = \sim 280$ K. This is supported by the isothermal magnetization curves, shown in Figure 5, which reveal the presence of a net magnetic moment below T_C. At 100 K, the magnetization increases rapidly at low

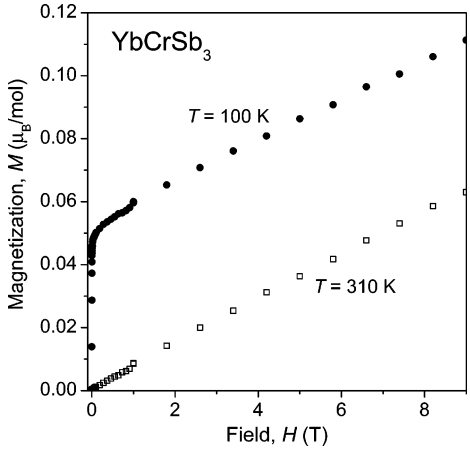

Figure 5. Isothermal magnetization of $YbCrSb_3$ at 100 and 310 K.

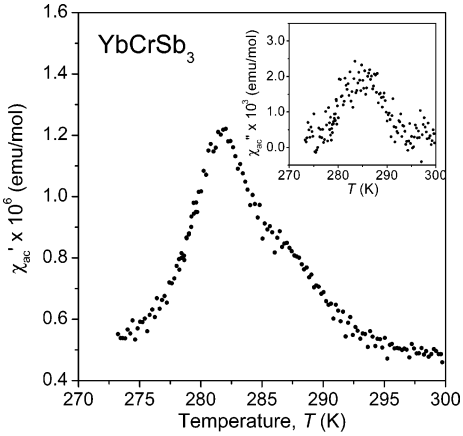

Figure 6. Real and imaginary (inset) components of the ac magnetic susceptibility of $YbCrSb_3$.

applied fields, but does not reach saturation up to 9 T. The magnetization values are quite low (0.11 μ_B/mol at 9 T), about an order of magnitude less than that found in $LaCrSb_3$. The maximum in the ac magnetic susceptibility curve, shown in Figure 6, pinpoints the transition temperature at 282 K, but there is also a nonzero imaginary component (shown in inset) that suggests the presence of uncompensated spin.

Discussion

$YbCrSb_3$ undergoes long-range magnetic ordering at a considerably higher temperature (by more than 100 K) than any other *RE*$CrSb_3$ member so far. There is strong evidence that Yb is present in its divalent state, implying an f^{14} configuration which would not contribute any localized moments to the overall magnetization. Because the only other member of the *RE*$CrSb_3$ series whose magnetism is governed solely by the presence of transition-metal moments is $LaCrSb_3$, it is appropriate to compare the behavior of these two compounds. Initial powder neutron diffraction studies on $LaCrSb_3$ suggested a bulk ferromagnetic structure originating from alignment of itinerant Cr moments.[5] Later, single-crystal neutron diffraction studies revealed the observation of weak reflections attributable to an antiferromagnetic spin sublattice.[10] The presence of a net magnetic moment in $LaCrSb_3$ is then the result of canted antiferromagnetic spin ordering leading to the formation of a weak ferromagnet with T_C of 126 K. The net moment resides along the *b* axis, with

a canting angle of 18° away from this axis, placing the easy magnetization axis perpendicular to the chains of face-sharing Cr-centered octahedra.[10] A similar model could account for the low saturation magnetization in $YbCrSb_3$, if the canting angle is even more pronounced. However, evidence of spin reorientation observed for $LaCrSb_3$ was not seen in $YbCrSb_3$. Because the $^{2}_{\infty}[CrSb_2]$ layers are quite far apart (at a separation equal to the *a* parameter, ~13 Å), the magnetic coupling interactions are much stronger within these layers than between them, as confirmed by single-crystal magnetization measurements on $LaCrSb_3$.[9] Because *a* contracts more rapidly than *b* or *c* on proceeding to the later *RE* members of *RE*$CrSb_3$, the higher T_C observed in $YbCrSb_3$ compared to $LaCrSb_3$ would then be consistent with a tendency toward a more three-dimensional magnetic structure.

If a naive, localized picture is envisioned for the bonding as occurring through full transfer of electrons from the *RE* and Cr atoms to the Sb substructure, and one-electron bonds ("half-bonds") are assumed for the ~3.0 Å Sb1−Sb2 and Sb3−Sb3 contacts, then a formulation such as $(RE^{3+})(Cr^{3+})(Sb^{2.5-})(Sb^{2.5-})(Sb^{1-})$ is a reasonable first approximation for the trivalent *RE* members. Continuing with this assumption, one could propose the formulation $(Yb^{2+})(Cr^{4+})(Sb^{2.5-})(Sb^{2.5-})(Sb^{1-})$ for $YbCrSb_3$. Given that the Cr−Sb bond lengths do not change significantly on going from $LaCrSb_3$ to $YbCrSb_3$, it is difficult to envision that there is a drastic change in the (localized) oxidation state of Cr. Although there has been debate about the relative importance of localized states of Cr in *RE*$CrSb_3$ compounds,[12] it seems possible that a change to a divalent state for the *RE* could be sufficient in itself to alter the distribution of itinerant Cr states to affect the net magnetic moment. To determine whether the Yb atoms are purely divalent will require a more careful analysis of the electronic structure.

A weakly ferromagnetic model is the most reasonable one to propose at this stage for $YbCrSb_3$, but further investigation is needed to clarify the detailed electronic and magnetic structure. We are optimizing the synthesis of $YbCrSb_3$ in preparation for neutron diffraction measurements. The hypothetical compound "$CaCrSb_3$", isoelectronic to $YbCrSb_3$, would also be worthwhile targeting.

Acknowledgment. The Natural Sciences and Engineering Research Council of Canada and the University of Alberta supported this work. We thank Dr. Robert McDonald (Faculty Service Officer, X-ray Crystallography Laboratory) for the X-ray data collection and Ms. Christina Barker (Department of Chemical and Materials Engineering) for assistance with the EDX analysis.

Supporting Information Available: Crystallographic information (CIF). This material is available free of charge via the Internet at http://pubs.acs.org.

CM0506151